Published in final edited form as:
Protein J. 2014 October ; 33(5): 403–409. doi:10.1007/s10930-014-9573-y.

The Role of Strong Electrostatic Interactions at the Dimer Interface of Human Glutathione Synthetase

Margarita C. De Jesus[a], **Brandall L. Ingle**[b], **Khaldoon A. Barakat**[b], **Bisesh Shrestha**[a], **Kerri D. Slavens**[a], **Thomas R. Cundari**[b], and **Mary E. Anderson**[a,*]

[a]Department of Chemistry and Biochemistry, Texas Woman's University, Denton, TX 76204, USA

[b]Center for Advanced Scientific Computing and Modeling (CASCaM), Department of Chemistry, University of North Texas, Denton, TX 76203, USA

Abstract

The obligate homodimer human glutathione synthetase (hGS) provides an ideal system for exploring the role of protein-protein interactions in the structural stability, activity and allostery of enzymes. The two active sites of hGS, which are 40 Å apart, display allosteric modulation by the substrate γ-glutamylcysteine (γ-GC) during the synthesis of glutathione, a key cellular antioxidant. The two subunits interact at a relatively small dimer interface dominated by electrostatic interactions between S42, R221, and D24. Alanine scans of these sites result in enzymes with decreased activity, altered γ-GC affinity, and decreased thermal stability. Molecular dynamics simulations indicate these mutations disrupt interchain bonding and impact the tertiary structure of hGS. While the ionic hydrogen bonds and salt bridges between S42, R221, and D24 do not mediate allosteric communication in hGS, these interactions have a dramatic impact on the activity and structural stability of the enzyme.

Keywords

Glutathione synthetase; glutathione; protein-protein interactions; negative cooperativity

1 Introduction

Protein-protein interactions facilitate numerous cellular processes in regulated pathways often modulated via conformational changes induced by protein-protein or protein-ligand interactions [1-3]. The importance of protein-protein interactions is particularly obvious in G-protein coupled receptors such as metabotropic transmembrane γ-aminobutyric acid receptors ($GABA_B$) and metabotropic glutamate receptors (mGluRs), where a ligand binds at one site and induces conformational and therefore functional changes at a distant site [4]. Such protein-protein interaction sites are increasingly pursued as drug targets in the treatment of cancers, autoimmune diseases, and bacterial infections [5,6]. Despite the passage of more than a century since the first experimental evidence of protein cooperativity, the atomic-level sequence of events that elucidate allostery remains a subject

*Corresponding author: Department of Chemistry and Biochemistry, Texas Woman's University, P.O. Box 425859, Denton, TX 76204. Phone: +1 940 898 2564, Fax: +1 940 898 2548. manderson3@mail.twu.edu.

of considerable debate [7-9]. The intersection of protein-protein interactions and protein cooperativity, particularly with regard to interchain salt bridges and hydrogen bonds, is an increasingly relevant area of study [10, 11].

The structural and kinetic properties of human glutathione synthetase (hGS) make it an ideal model for exploring protein-protein interactions. An obligate homodimer with C_2 symmetry, hGS has distant active sites (40 Å apart) separated by a relatively small dimer interface. Each active site catalyzes the second step in the biosynthesis of the key antioxidant glutathione (GSH) through the ATP dependent ligation of γ-glutamylcysteine (γ-GC) and glycine [12]. The enzyme is negatively cooperative towards its γ-glutamyl substrate; thus, when the first γ-GC substrate binds, the substrate affinity of the second subunit of hGS decreases [13]. The allostery of hGS likely mediates the flux of γ-GC, while maintaining cellular levels of GSH [14, 15]. Communication between the active sites of hGS may pass through the dimer interface. The current study of the dimer region of hGS, particularly the electrostatic interactions across the interface, may provide crucial information on the role of protein-protein interactions in maintaining the tertiary structure of the enzyme and the origins of allosteric communication.

Structurally, hGS is similar to other members of the ATP-grasp superfamily of enzymes with a characteristic ATP-grasp fold, which aids in the ATP driven formation of a carbon-nitrogen bond [16]. As one of the few mammalian ATP-grasp enzymes whose crystal structure is known, hGS provides insight into the structural and functional similarities, as well as differences, between mammalian and prokaryotic ATP-grasp enzymes, which are often targeted by antibiotics [17]. Regulation of hGS also plays a critical role in maintaining the cellular glutathione levels required to relieve oxidative stress. Patients with genetic deficiencies in hGS suffer from a variety of symptoms, most notably hemolytic anemia and neurological disorders [18]. Deficiencies of GSH are associated with a variety of diseases including Parkinson's disease, Alzheimer's disease, Lou Gehrig's disease, diabetes, cystic fibrosis, and HIV/AIDS [19-21]. A better understanding of hGS regulation may elucidate the precise relationship between GSH and these disease states.

Recent research on the hydrophobic interactions of V44 and V45 at the interface of hGS highlights the importance of this region in both allostery and stability [22]. All V44/45 mutations resulted in decreased activity, decreased negative cooperativity, and decreased thermal stability relative to wild-type hGS [22]. The remarkable finding that V44 and V45 lie along the allosteric pathway of hGS and that disruption of the hydrophobic interactions at this site impacts the global geometry of hGS invites further study into dimer interface interactions.

In the current work, computational analysis of hGS indicates that the amino acids S42 and R221 participate in electrostatic interactions with D24 across the dimer interface (separations < 3.0 Å). The strength of these interactions, relative to the hydrophobic interactions at V44 and V45, suggests that these residues may be crucial to function of hGS. Since D24 participates in two significant interactions (a salt bridge with R221 and an ionic hydrogen bond with S42), it is reasonable to hypothesize that this residue plays the largest role in hGS activity and stability. The present research delineates the function of dimmer

interface interactions between S42, R221, and D24 in terms of the activity, cooperativity and stability of hGS.

2 Materials and Methods

2.1 Materials

Expression vector pET-15b, *E. coli* XL1 Blue competent cells, and Ni-NTA His-Bind® resin were from Novagen, Inc. The primers were synthesized by Integrated DNA Technologies, Inc. The QuickChange™ Site-Directed Mutagenesis Kit and Wizard® *Plus* Midipreps DNA Purification System were obtained from Stratagene, Inc. and Promega, respectively. American Bioanalytical, Inc. supplied the isopropyl-1-thio-β-galactopyranoside (IPTG). L-γ-glutamyl-L-α-aminobutyrate (γ-GluABA) was synthesized [13] or obtained from Bachem, Inc. Protein concentrators were from Pierce, Inc. All other reagents, unless noted, were of high purity and obtained from Sigma-Aldrich, US Biological, Fisher Scientific or Amresco.

2.2 Preparation of hGS mutant enzymes

Wild-type hGS in pET-15b expression vector has an N-terminal 6x histidine tag (hGS-pET-15b [23-25]). PCR/site-directed mutagenesis was carried out with internal primers (Table S1, Online Resources). The hGS wild-type and mutant cDNA sequences were confirmed by sequencing (GENEWIZ, Inc.). The hGS-pET-15b plasmid DNAs were expressed in *E. coli* BL21(DE3) cells [23, 24].

2.3 Purification

Wild-type and mutant enzymes were purified from *E. coli* BL21(DE3) cells as previously reported [22] with all procedures conducted at 4 °C. The purified hGS enzymes were dialyzed overnight in Tris buffer (20 mM Tris-Cl and 1 mM EDTA, pH 8.6). Enzymes were stored in sterile cryogenic tubes in the Tris buffer at 4 °C. Purity was determined by SDS-PAGE [22, 23]. Protein concentration was determined using the Lowry method [26], with bovine serum albumin as standard.

2.4 Enzyme Assays and Kinetic Analysis

The activity of purified hGS enzymes was measured using a pyruvate kinase (PK)/lactate dehydrogenase (LDH) coupled assay as previously described [22-24]. To avoid complications of oxidation of the γGC thiol, γ-GluABA, an analog of γ-GC with the same activity and kinetic properties as γGC, was used [13]. Reactions were initiated upon addition of purified recombinant hGS to a pre-incubated (11 mins) standard reaction mixture of 100 mM Tris (pH 8.2, 25 °C), 50 mM KCl, 20 mM $MgCl_2$, 5 mM PEP, 10 units/assay LDH (type II rabbit muscle), 10 units/assay PK (type II rabbit muscle), and 0.3 mM NADH with a final volume of 0.2 mL. The concentrations of γ-GluABA, ATP and glycine were each 10 mM for specific activity measurements. The reaction rate was monitored continuously at 340 nm. An enzyme unit is defined as amount of enzyme needed to catalyze the formation of 1 μmol of product/min at 37.0 °C.

Kinetic parameters (K_m, Hill Coefficients) were determined using the standard assay above with varying concentrations of γ-GluABA to at least 10-fold above and below the approximate K_m while keeping the concentration of glycine and ATP constant. Control reactions were run in the absence of γ-GluABA. Sigma Plot 11.0 software was used to calculate and determine Hill coefficients, K_m and V_{max} [24, 26].

2.5 Differential Scanning Calorimetry (DSC)

Enzymes were dialyzed overnight in Tris buffer (above) and concentrated to 1.0-2.0 mg/mL [22]. Scans were carried out (Calorimetry Sciences Nano Series III, 1.0 atm, rate of 1.0 °C/min, 10 - 90 °C) and baseline corrected against dialysate after being degassed (15 min).

2.6 Circular Dichroism

Enzymes were dialyzed overnight in sodium phosphate buffer (10 mM, pH 7.5, 2 × 1 L, 4 °C). Measurements were carried out on an OLIS RSM 1000 with DSM CD attachment (260 to 190 nm) as previously described using OLIS GlobalWorks software for analysis [25]. Data was converted to molar ellipticity (deg cm^2 $dmol^{-1}$) and represent an average of at least 5 scans.

2.7 Computational Methods

A combination of bioinformatics, *ab initio* calculations, and molecular dynamics was used to computationally probe the sequence and structure of hGS. A complete description of computational methods is found in the Online Resources. The techniques used were similar to previously published work on hGS [22, 23, 28].

3 Results

3.1 Analysis of Dimeric hGS Crystal Structure

Analysis of dimeric hGS was initiated by mapping all strong contacts between chain A and chain B within the crystal structure of hGS (2HGS) [29]. The number of residues close to the dimer interface falls off rapidly as the threshold distance is reduced, with only 5 residues per monomer having interchain distances < 3.0 Å. The five residues with the most significant bonding across the dimer interface (D24, S42, E43, Y47, and R221) were considered initial targets for study. These five residues participate in three significant interactions across the interface (S42···D24, Y47···E43, R221···D24). Molecular dynamics simulations indicate that the Y47···E43 interaction is more easily disrupted and thus less important than the others; see Section 2.7 and the Online Resources for full details. Hence, further study focuses primarily on the S42···D24, and R221···D24 interactions.

3.2 Sequence Analysis

Sequence alignment of hGS compared to glutathione synthetase of higher eukaryotes and mammals shows moderate overall sequence identity, 43% and 71%, respectively (Table 1). Among mammals the polar residues S42, R221 and D24 have sequence conservation comparable to the hydrophobic dimer interface residues V44 (67%) and V45 (62%), which were shown in previous research to be important in allostery and stability [22]. The mammalian conservations of S42 (62%), R221 (71%), and D24 (71%) suggest a genetic

drive across species to retain those residues at these locations, especially in the case of R221 and D24.

3.3 Ab Initio Calculations of Amino Acid Interactions

The interaction energies from *ab initio* residue:residue calculations show that the medium of the calculation (*cf*. gas-phase and aqueous) has significant impact (Fig 1). Solvent shielding in aqueous systems is substantial, particularly on the R221···D24 salt bridge. Hence, solvent molecules (*in vivo* or *in vitro*) and solvent polarity can drastically attenuate dimer interface interactions in hGS. Additionally, the calculated salt bridge (R221···D24) interaction energy in an aqueous environment is double the binding energy of the hydrogen bond at S42···D24 (-13.5 vs. -6.1 kcal/mol), suggesting that the salt bridge contact is the more substantial. As D24 participates in both a strong salt bridge with R221 and a strong hydrogen bond with S42, it may serve a key role in the interchain interactions of hGS.

3.4 Experimental Activity and Kinetic Studies of hGS Mutant Enzymes

The functional effects of dimer interface mutations, S42A, R221A and D24A, relative to wild-type (WT) hGS were assessed by activity: k_{cat} (s^{-1}) = 15.6, 13.5, 11.9, and 18.2 (WT), respectively. These mutations lead to lower activity (by ∼ 15 - 35%) than wild-type hGS when measured immediately after (within a few hours) purification (Table 2). Wild-type hGS displays negative cooperativity toward its γ-glutamyl substrate (γ-GluABA) with a Hill coefficient of 0.69 [27]. The mutant hGS dimer interface enzymes prepared here have nearly identical Hill coefficients (0.68 to 0.72) (Table 2). Thus, rather surprisingly, the three dimer interface residues involved in electrostatic interactions lower the k_{cat} of the enzyme without significantly impacting negative cooperativity in hGS.

The γ-GluABA Michaelis constant (K_m) represents the γ-GluABA concentration where the reaction rate is half of V_{max}, and relates to substrate affinity. The wild-type hGS, S42A, R221A and D24A have K_m values of 1.31, 0.95, 0.68 and 0.71 mM, respectively (Table 2). The apparent increase in affinity for γ-GluABA exhibited by the K_m of these dimer interface mutants is due to tighter substrate binding, possibly coupled with a decrease in rates of product formation and substrate dissociation. Compared to wild-type there is a slight increase in catalytic efficiency (k_{cat}/K_m) of the dimer interface mutants S42A, R221A and D24A (Table 2). Therefore, hGS residues (S42, R221 and D24) that have hydrogen bonding and ionic interactions across the dimer interface decrease activity, maintain negative cooperativity, increase γ-GluABA affinity, and increase catalytic efficiency when mutated to alanine.

3.5 Temporal Analysis of Enzyme Activity

While wild-type hGS is stable for several years when stored in a Tris-Cl buffer (20 mM Tris-Cl and 1 mM EDTA, pH 8.6) in sterile cryogenic tubes at 4 °C, the hGS dimer interface mutant enzymes lost activity in the 30 hours after purification. Both R221A and D24A lost activity in a biphasic manner (Fig 2) within a few hours; D24A lost 30% of activity in 4 hours, while R221A activity decreased by 20% in 7.5 hours. Interestingly, despite different initial activities, both R221A and D24A plateaued at a similar k_{cat} (∼ 8 s^{-1}). Several hGS mutants have exhibited the temporal shift in activity [20, 25]. While MD simulations do not

allow for models on such long time scales, it is likely that the disrupted interchain bonding in D24A and R221A results in a gradual loss in activity as the mutant enzymes denature. The plateaus in activity may represent a point at which the enzymes reach a new structural equilibrium. In contrast, the S42A mutant was fairly stable, with a 10% loss in activity in 3 days and a 40% drop in activity after 6 weeks (data not shown). All three dimer interface hGS mutants lose activity over time, an exceptionally fast change in the case of R221A and D24A.

3.6 Experimental Measurement of Stability and Secondary Structure

Differential scanning calorimetry (DSC) was used to compare enzyme stability. Wild-type hGS has an unfolding or transition midpoint (T_m) of 60.3 °C. The T_m values of S42A, R221A and D24A are 49.7, 42.5 and 39.3 °C, respectively (Table 2). The stability of each hGS mutant enzyme decreased compared to wild-type, supporting computational predictions of the importance of these residues from the conservation and structural analyses (*vide supra*).

The wild-type hGS circular dichroism (CD) spectrum shows distinct negative bands of molar ellipticity around 212 and 225 nm. The S42A and R221A mutant hGS enzymes have CD spectra similar to wild-type. The CD spectrum of D24A shows the largest loss of negative molar ellipticity, around 208 nm (Fig S2, Online Materials).

3.7 RMSD Analysis of Molecular Dynamics Geometries

The structural alignment of S42A, R221A and D24A with wild-type hGS (all are the lowest-energy structures obtained from MD simulations) resulted in average root mean square deviations (RMSD) of 1.24, 1.88 and 1.25 Å, respectively (Table S2, Online Materials). Although the D24A and S42A mutants showed similar movement within the protein as a whole, the S42A mutation had a larger impact on the dimer region geometry. Of the mutants studied, R221A exhibited the largest RMSD both within the dimer region and the entire protein, indicating conformational change.

3.8 Hydrogen Bond Analysis of Molecular Dynamics Geometries

A summary of all bonds within 4.5 Å of S42, R221 and D24 within the wild-type and mutant hGS enzymes elucidates the structural significance of these residues (Table S3 in Online Resources, the two subunits are designated “a” and “b”). In the wild-type there are six significant electrostatic interactions across the two chains: two ionic hydrogen bonds and a salt bridge between D24 and R221, two ionic hydrogen bonds between D24 and S42, and one ionic hydrogen bond between E43b and S46a. A comprehensive list of intrachain interactions is given in Table S3.

Intrachain bonding is largely unaffected by the D24A mutation, Table S3. Upon D24A mutation, two symmetrical interchain hydrogen bonds between residues E43 and S46 remain but all of the other surrounding intrachain hydrogen bonds are disrupted, Fig 3. Although the mutation of S42A disrupts some interchain interactions, it also creates new interchain hydrogen bonds (Table S3, Fig S3, Online Resources), consistent with the moderate drop in activity. A salt bridge (D24-R34) and an interchain hydrogen bond (S46-A42) form in the

S42A mutant in place of the S42-D24, and S42-E43 interchain bonds of the wild-type enzyme, Fig S3. In the R221A mutant, the interchain salt bridge and hydrogen bonds between R221 and D24 are broken, and a new salt bridge forms between R34 and D24. The R221A mutation also has a large impact on the intrachain bonding structure (Table S3, Fig S4, Online Resources). Overall, the R221A mutation results in a moderate loss of interchain bonds, when compared with the dramatic drop in interchain bonds in the D24A mutant and the small shift in interchain bonds in the S42A mutant, Table S3.

4 Discussion

Computational analysis of the dimer interface of hGS indicated that electrostatic interactions between S42, D24, and R221 dominated subunit:subunit interactions. An initial hypothesis posited that these interactions may stabilize the obligate homodimer and affect the allostery of the negatively cooperative enzyme. Alanine scans of these residues (S42A, R221A, and D24A) and MD simulations of the mutants were conducted to assess the impact on activity, stability and cooperativity.

Molecular dynamics simulations indicate that while alanine mutations of S42, R221, and D24 impact the overall conformation of hGS (Table S2), these mutations primarily disrupt the strong ionic salt bridges and hydrogen bonds across the dimer interface. The number and strength of interchain bonds lost directly correlates to the observed drop in thermal stability (T_m). This change in secondary structure is mirrored by small changes in the CD spectra of the mutant enzymes relative to wild-type hGS. Upon loss of the strong dimer interface interactions, the vibrational freedom of the mutant proteins increases, allowing for greater motion, and therefore decreased stability, within the entire enzyme. Indeed, the present research in conjunction with previous studies of V44/45 [22] infers that hGS is an obligate dimer. All experimental and computational studies show that the mutation at D24 results in the greatest loss of interchain bonds and the most dramatic variation in overall structure.

The activity of the dimer interface mutants (S42A > R221A > D24A) also parallels the loss of interchain bonds (Fig. 1, Fig. 3). The rapid drops in activity over time exhibited by the D24A and R221A mutants, coupled with the moderate temporal drop in activity for S42A (Fig. 2) further support the role of interchain interactions in the function of the enzyme. The reduced enzyme stability may also impact the activity of the mutations, especially in D24A. With two strong electrostatic interactions at the interface, D24 plays the most pivotal role in maintaining hGS activity.

Kinetic studies of dimer interface mutants (S42A, R221A, and D24A) show that changes at the interface have a long distance impact on the active site of hGS. The Michaelis constant (K_m) for γ-GluABA decreased upon mutation of these residues, which may explain the drops in activity exhibited by these mutants. While the mutant enzymes may bind γ-GluABA better than wild-type, the reaction does not proceed to product as quickly. Notably, the Hill coefficients of S42A, R221A, and D24A were similar to wild-type, indicating that these mutations do not alter the negative cooperativity of hGS. The low Michaelis constants and negligible changes in Hill coefficients suggest that while S42, R221, and D24 do not lie

along the allosteric pathway, these residues remain important for the activity and stability of the enzyme.

In conclusion, the present research on homodimeric hGS implies that strong electrostatic interactions are essential for the stability of multimeric enzymes, but need not necessarily mediate allosteric communications. Alternatively, weaker chemical bonding phenomena, *e.g.*, hydrophobic interactions [22], may provide a more flexible (chemically and evolutionarily) communication pathway between enzyme active sites separated by long distances. By extension, allosteric pathways in enzymes may arise not from a few strong chemical bonds, but rather a “conspiracy” among larger numbers of weaker interactions. Perhaps the polar dimer interface residues do not modulate cooperativity, because the disruption of strong electrostatic interactions across the protein-protein interface has such a drastic impact on the functional stability of hGS. Studies are currently underway in our laboratory to further delineate the allosteric pathways and protein-protein interactions of hGS, providing the essential data needed to test the various models of protein allostery and interaction.

Supplementary Material

Refer to Web version on PubMed Central for supplementary material.

Acknowledgments

The authors thank the Chemical Computing Group for providing the MOE software. We also thank Amy Graves, Teresa Brown, and Sarah Barelier for technical assistance and Mark Britt and Richard Sheardy for instrumentation assistance. Supported in part by NIH R15GM086833 (MEA), a Research Enhancement Program Grant (TWU, MEA), and a UNT Faculty Research Grant (TRC).

References

1. Haber JE, Koshland DE Jr. Relation of protein subunit interactions to the molecular species observed during cooperative binding of ligands. Proc Natl Acad Sci USA. 1967; 58:2087–2093. [PubMed: 5237502]
2. Kirtley ME, Koshland DE Jr. Models for cooperative effects in proteins containing subunits. Effects of two interacting ligands. J Biol Chem. 1967; 242:4192–4205. [PubMed: 4294047]
3. Kantrowitz ER. Allostery and cooperativity in Escherichia coli aspartate transcarbamoylase. Arch Biochem Biophys. 2012; 519:81–90. [PubMed: 22198283]
4. May LT, Leach K, Sexton PM, Christopoulos A. Allosteric modulation of G-protein coupled receptors. Annu Rev Pharmacol Toxicol. 2007; 47:1–51. [PubMed: 17009927]
5. Geitmann M, Elinder M, Seeger C, Brandt P, de Esch IWJ, Danielson UH. Identification of a novel scaffold for allosteric inhibition of wild type and drug resistant HIV-1 reverse transcriptase by fragment library screening. J Med Chem. 2011; 54:699–708. [PubMed: 21207961]
6. Wells JA, McClendon CL. Reaching for high hanging fruit in drug discovery at protein-protein interfaces. Nature. 2007; 450:1001–1009. [PubMed: 18075579]
7. Bohr C, Hasselbach KA, Krogh A. Skan. Arch Physiol. 1904; 16:402–412.Koshland DE Jr, Hamadani K. Proteomics and models for enzyme cooperativity. J Biol Chem. 2002; 277:46841–46844. quoted in. [PubMed: 12189158]
8. Kalodimos CG. Protein function and allostery: a dynamic relationship. Ann NY Acad Sci. 2012; 1260:81–86. [PubMed: 22256894]
9. Rader AJ, Brown SM. Correlating allostery with rigidity. Mol Biosyst. 2011; 7:464–471. [PubMed: 21060909]

10. Jones S, Thornton JM. Principles of protein-protein interactions. Pro Natl Acad Sci USA. 1996; 93:13–20.
11. Keskin O, Gursoy A, Ma B, Nussinov R. Principles of protein-protein interactions: what are the preferred ways for proteins to interact? Chem Rev. 2008; 108:1225–1244. [PubMed: 18355092]
12. Meister A, Anderson ME. Glutathione. Annu Rev Biochem. 1983; 52:711–760. [PubMed: 6137189]
13. Oppenheimer L, Wellner VP, Griffith OW, Meister A. Glutathione synthetase purification from rat kidney and mapping of the substrate binding sites. J Biol Chem. 1979; 254:5184–5189. [PubMed: 447639]
14. Bush EC, Clark AE, DeBoever CM, Haynes LE, Hussain S, Ma S, McDermott MM, Novak AM, Wentworth JS. Modeling the role of negative cooperativity in metabolic regulation and homeostasis. PLoS One. 2012; 7:e48920. [PubMed: 23152821]
15. Cornish-Bowden A. The physiological significance of negative cooperativity revisited. J Theor Biol. 2013; 319:144–147. [PubMed: 23261394]
16. Galperin MY, Koonin EV. A diverse superfamily of enzymes with ATP-dependent carboxylate-amine/thiol ligase activity. Protein Sci. 1997; 6:2639–2643. [PubMed: 9416615]
17. Fawaz MV, Topper ME, Firestine SM. The ATP-grasp enzymes. Bioorg Chem. 2011; 39:185–191. [PubMed: 21920581]
18. Ristoff R, Larsson A. Oxidative stress in inborn errors of metabolism: lessons from glutathione deficiency. J Inherit Metab Dis. 2002; 25:223–226. [PubMed: 12137231]
19. Bains JS, Shaw CA. Neurodegenerative disorders in humans: the role of glutathione in oxidative stress-mediated neuronal death. Brain Res Rev. 1997; 25:335–358. [PubMed: 9495562]
20. Larsson, A.; Ristoff, E.; Anderson, ME. Glutathione synthetase deficiency and other disorders of the γ-glutamyl cycle. In: Scriver, CR.; Beaudet, AL.; Sly, WS.; Valle, D., editors. Metabolic Basis of Inherited Disease. McGraw Hill; New York: 2005. Online (genetics.accessmedicine.com)
21. Townsend DM, Tew KD, Tapiero H. The importance of glutathione in human disease. Biomed Pharmacother. 2003; 57:145–155. [PubMed: 12818476]
22. Slavens KD, Brown TR, Barakat KA, Cundari TR, Anderson ME. Valine 44 and valine 45 of human glutathione synthetase are key for subunit stability and negative cooperativity. Biochem Biophys Res Commun. 2011; 410:597–601. [PubMed: 21683691]
23. Dinescu A, Cundari TR, Bhansali VS, Luo JL, Anderson ME. Function of conserved residues of human glutathione synthetase. J Biol Chem. 2004; 279:22412–22421. [PubMed: 14990577]
24. Dinescu A, Brown TR, Barelier S, Cundari TR, Anderson ME. The role of the glycine triad in human glutathione synthetase. Biochem Biophys Res Commun. 2010; 400:511–516. [PubMed: 20800579]
25. Brown TR, Drummond ML, Barelier S, Crutchfield AS, Dinescu A, Slavens KD, Cundari TR, Anderson ME. Aspartate 458 of human glutathione synthetase is important for cooperativity and active site structure. Biochem Biophys Res Comm. 2011; 411:536–542. [PubMed: 21771585]
26. Lowry OH, Rosebrough NJ, Farr AL, Randall RJ. Protein measurement with the folin phenol reagent. J Biol Chem. 1951; 193:265–275. [PubMed: 14907713]
27. Luo JL, Huang CS, Babaoglu K, Anderson ME. Novel kinetics of mammalian glutathione synthetase: characterization of gamma-glutamyl substrate cooperative binding. Biochem Biophys Res Commun. 2000; 275:577–581. [PubMed: 10964706]
28. Dinescu A, Anderson ME, Cundari TR. Catalytic loop motion in human glutathione synthetase: a molecular modeling approach. Biochem Biophys Res Commun. 2007; 353:450–456. [PubMed: 17188241]
29. Polekhina G, Board PG, Gali RR, Rossjohn J, Parker MW. Molecular basis of glutathione synthetase deficiency and a rare gene permutation event. EMBO J. 1999; 12:3204–3213. [PubMed: 10369661]

Abbreviations

hGS	human glutathione synthetase
GSH	glutathione
γ-GC	γ-glutamylcysteine
γ-GluABA	L-γ-glutamyl-L-α-aminobutyrate
IPTG	isopropyl-1-thio-β-galactopyranoside
PK	pyruvate kinase
LDH	lactate dehydrogenase
DSC	differential scanning calorimetry
2HGS	crystal structure of human glutathione synthetase
WT	wild-type
T_m	transition midpoint
MD	molecular dynamics
RMSD	root mean square deviation

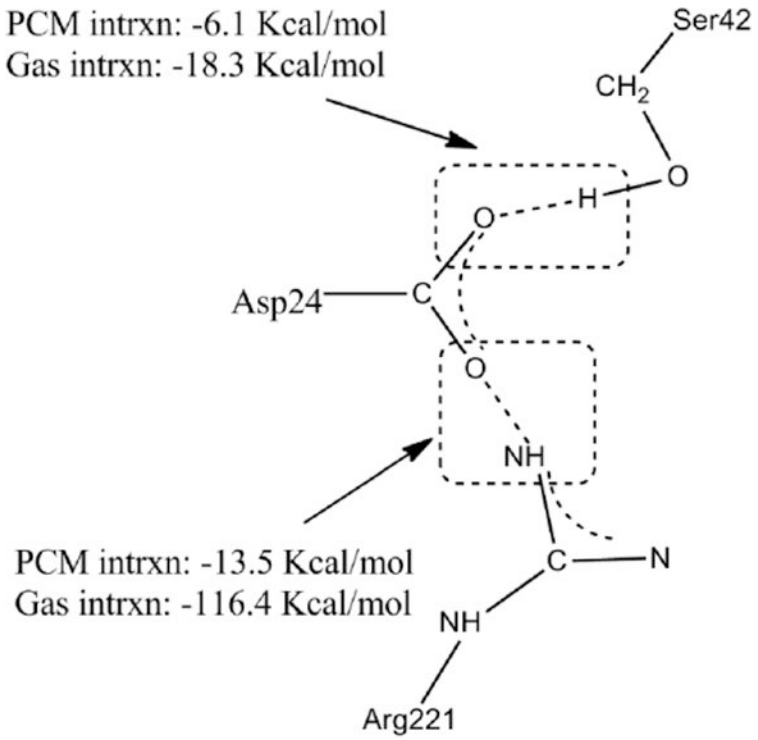

Fig 1.

Interaction energies across the dimer interface of hGS. Calculated with B3LYP/6-31+G(d) for amino acids S42, R221 and D24 across the dimer interface of *hGS* in the gas and PCM (aqueous) phase

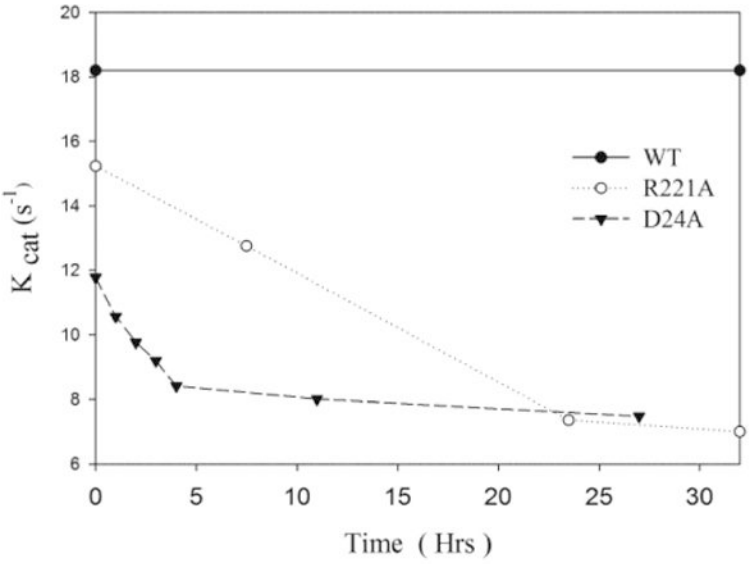

Fig 2.

Activity of wild-type and hGS mutant enzymes R221A and D24A over time. Values represent an average of two assays of at least two independent purifications (per enzyme). Enzymes were stored in sterile cryogenic tubes in Tris-Cl buffers (20 mM Tris-Cl and 1 mM EDTA, pH 8.6) at 4 °C.

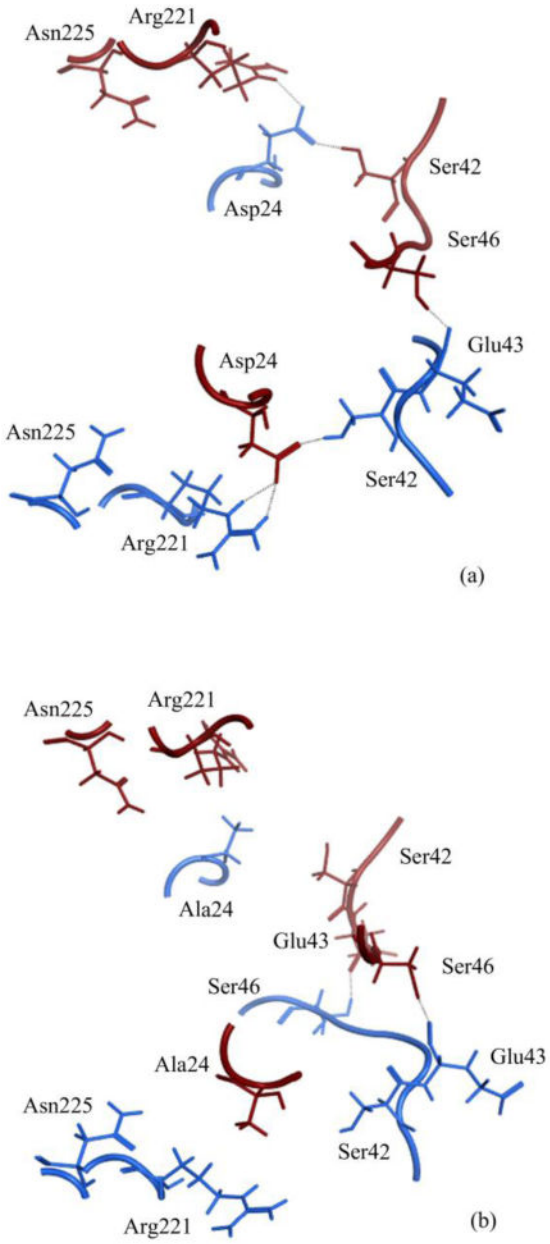

Fig 3.

Hydrogen bonding in (a) wild-type hGS and (b) D24A hGS. Chain A is in red (dark) and chain B is in blue (light)

Table 1

Comparison of the conservation of hGS residues near the dimer interface between higher eukaryotes and mammals

	Higher Eukaryotes*		Mammals	
Residue	**%C**	**%CC**	**%C**	**%CC**
D24	63.4	64.6	71.4	71.4
S42	24.4	59.8	61.9	66.7
E43	7.3	14.6	23.8	52.4
V44	39.0	51.2	66.7	76.2
V45	15.9	51.2	61.9	76.2
Y47	22.0	81.7	81.0	81.0
R221	40.2	40.2	71.4	71.4
Ave	42.6	60.3	70.5	76.0
St Dev	18.2	19.8	17.3	11.2

*Higher eukaryotes include species from the Plantae and Animalia kingdoms; %C = conservation; %CC = charge conservation (positive, negative or neutral); Ave = average conservation for all amino acids relative to hGS. St Dev = sample standard deviation.

Table 2

Activity, kinetic properties and thermal stability of hGS

Enzyme	k_{cat} (s^{-1})	K_m (mM)	k_{cat}/K_m (s^{-1} mM^{-1})	Hill Coef.	T_m (°C)
WT	18.2 ± 2.0 (100%)	1.31 ± 0.13	1.39×10^{-4}	0.69 ± 0.03	60.3 ± 0.3
S42A	15.6 ± 0.5 (85%)	0.95 ± 0.08	1.64×10^{-4}	0.72 ± 0.06	49.7 ± 0.1
R221A	13.5 ± 3.0 (74%)	0.68 ± 0.08	1.99×10^{-4}	0.68 ± 0.04	42.5 ± 0.4
D24A	11.9 ± 0.3 (65%)	0.71 ± 0.02	1.68×10^{-4}	0.68 ± 0.05	39.3 ± 0.1

* Duplicate assays carried out on 2 - 3 independent purifications (per enzyme) so that n = 4 - 6.

Protein J. Author manuscript; available in PMC 2015 October 01.